Liquid Crystals
Publication details, including instructions for authors and subscription information:
http://www.tandfonline.com/loi/tlct20

Influence of the backward propagating waves on the twist optical Fréedericksz transition in planar nematic films

Dmitry O. Krimer [a b], Andrey E. Miroshnichenko [c] & Etienne Brasselet [d]

[a] Max Planck Institute for the Physics of Complex Systems, Dresden, Germany

[b] Theoretische Physik, Universität Tübingen, Tübingen, Germany

[c] Nonlinear Physics Centre and Centre for Ultra-high bandwidth Devices for Optical Systems (CUDOS), Australian National University, Canberra, Australia

[d] Université Bordeaux, LOMA, CNRS UMR 5798, F-33400, Talence, France

Available online: 12 Aug 2011

To cite this article: Dmitry O. Krimer, Andrey E. Miroshnichenko & Etienne Brasselet (2011): Influence of the backward propagating waves on the twist optical Fréedericksz transition in planar nematic films, Liquid Crystals, 38:8, 1021-1026

To link to this article: http://dx.doi.org/10.1080/02678292.2011.593197

Liquid Crystals,
Vol. 38, No. 8, August 2011, 1021–1026

Taylor & Francis
Taylor & Francis Group

Influence of the backward propagating waves on the twist optical Fréedericksz transition in planar nematic films

Dmitry O. Krimer[a,b*], Andrey E. Miroshnichenko[c] and Etienne Brasselet[d]

[a]*Max Planck Institute for the Physics of Complex Systems, Dresden, Germany;* [b]*Theoretische Physik, Universität Tübingen, Tübingen, Germany;* [c]*Nonlinear Physics Centre and Centre for Ultra-high bandwidth Devices for Optical Systems (CUDOS), Australian National University, Canberra, Australia;* [d]*Université Bordeaux, LOMA, CNRS UMR 5798, F-33400, Talence, France*

(*Received 16 February 2011; final version received 30 May 2011*)

We report on the influence of backward propagating waves on the twist optical Fréedericksz transition when a linearly polarised light impinges at normal incidence on a nematic liquid crystal film with planar alignment. We show that the reorientation threshold oscillates as a function of the optical thickness of the nematic layer. The amplitude of these oscillations strongly depends on the refractive index changes at the film boundaries and is shown to be related to interferential effects between forward and backward propagating waves that arise from unavoidable dielectric permittivity tensor mismatch and the film boundaries.

Keywords: nematic liquid crystals; Fréedericksz transition; orientational transitions; nonlinear optics

1. Introduction

Many aspects of complex light-induced nonlinear orientational phenomena in liquid crystals have been investigated during the last few decades, with a particular emphasis on the dynamical richness arising from the strong light–matter coupling associated with the elastic and anisotropic optical properties of ordered mesophases [1–3]. From the optical point of view, nematics are uniaxial media described by a local optical axis along the local average direction of the molecular axis called the director, **n**. Depending on the boundary conditions and bulk ordering characteristics, a light-driven orientational instability may take place above a threshold intensity usually referred to as the optical Fréedericksz transition (OFT). Besides their fundamental interest, the optically induced phenomena in liquid crystals seem to find their potential by moving towards technological applications. For instance, it has been recently proposed that all-optical photonic switching devices might be realised using dielectric periodic structures partially infiltrated with nematics [4–6].

When considering a linearly polarised light field impinging at normal incidence onto a planar nematic film, where the uniform director at rest lies in the plane of the film, the polarisation plane of the incident light is a key parameter. Usually, one considers the two situations when the electric field is parallel or perpendicular to the director at rest. In both cases, twisted elastic reorientation modes appear above a light intensity threshold. In the first case – extraordinary incident light – a coherent polarisation conversion process takes place. The latter is mediated by the coupling between the incident extraordinary (e) wave and a lower-frequency noisy ordinary component that arises from scattering of the incident light by the director orientational fluctuations. As a result, the ordinary (o) wave experiences gain during its propagation throughout the cell [7, 8]. In the second case – ordinary incident light – the twist optical Fréedericksz transition (TOFT) takes place. Up until now, this phenomenon has only been considered theoretically, which is explained by the predicted intensity threshold values that turn out to be very high [9]. Recently, the TOFT has been revisited and it has been shown that the stationary bifurcation solution derived by Santamato *et al.* [9] is only valid in the limit of optically thin nematic films. Indeed, for thick enough films, the TOFT takes place via a Hopf bifurcation [10]. Although experimental information is lacking, as said above, we note that the planar geometry has, nevertheless, been investigated experimentally by using a nematic film embedded into a periodic dielectric structure [11], which seemingly demonstrates the observation of an accessible intensity threshold in practice.

In this work, in an attempt to guide future experimental investigations, we quantitatively estimate the influence of unavoidable backward and forward light scattering from refractive indices mismatch at

*Corresponding author. Email: dmitry.krimer@gmail.com

ISSN 0267-8292 print/ISSN 1366-5855 online

DOI: 10.1080/02678292.2011.593197
http://www.informaworld.com

the boundaries of a realistic sample on the TOFT threshold. Such considerations are usually neglected, which is well justified for homeotropic alignment when the director is perpendicular to the plane of the film. However, in the case of planar alignment, matching the refractive indices at the boundaries imposes the use of anisotropic substrates, which have not been used in the OFT experiments reported so far. Our analysis unveils the crucial role of backward waves in the calculation of the threshold intensity value.

2. The model

We consider a linearly polarised plane wave with wavelength λ impinging at normal incidence (along z) on a planar aligned nematic liquid crystal layer of thickness L (see Figure 1). The unperturbed director, $\mathbf{n}_0$, lies along the x-axis and the light is polarised along the y-direction, i.e. we deal with an incident ordinary wave. The theoretical description of optically induced orientational phenomena in nematics is a well-posed problem that consists of coupled nemato-dynamic and Maxwell's equations for the light propagation inside an anisotropic medium [12]. There are several common simplifications that are employed to solve these equations. First, fluid flow associated with the director reorientation (backflow effect) is neglected. Indeed, flow plays only a passive role and in most known cases it merely leads to slight quantitative differences [13, 14]. In this study we neglect all transverse effects and assume that all variables depend solely on z. This allows us to simplify Maxwell's equations drastically. Therefore, a light beam in a real situation might be treated as a plane wave and any experimental

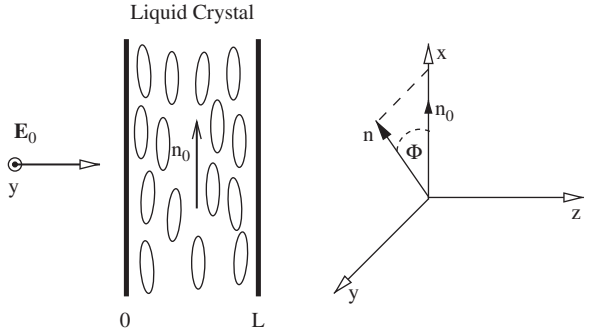

Figure 1. Light–matter interaction geometry: a linearly polarised light along the y-axis is normally incident onto a nematic layer with initial uniform alignment of the director, $\mathbf{n}_0$, along the x-axis. We refer to such an unperturbed state as the 'planar state'. Within the infinite plane wave approximation used in the present work, the reoriented liquid crystal is fully described by the dependence of the twist angle on the z coordinate and time (t), $\Phi(z, t)$.

attempt to validate the theoretical predictions should be performed by using a laser beam with a characteristic diameter much larger than the thickness of the nematic layer. The applicability of such a one-dimensional approximation has already been validated for homeotropic nematic samples, where $\mathbf{n}_0$ is parallel to the z-axis. More precisely, it turns out that this approximation also works rather well for the beam diameters of the order of approximately L [15, 16]. We note that the realisation of spatially inhomogeneous transverse structures in the (x, y) plane is hardly probable. Indeed, as shown in [17] in the limit of thin layers, such structures appear only for large elastic anisotropy, which is not the case for common nematics. Next, we assume strong anchoring conditions $\mathbf{n}(z = 0, t) = \mathbf{n}(z = L, t) = \mathbf{n}_0$ and introduce the representation adapted to our geometry in terms of the spherical angles $\Theta(z, t)$ and $\Phi(z, t)$, $\mathbf{n} = (\cos\Phi \sin\Theta, \sin\Phi \sin\Theta, \cos\Theta)$. However, as follows from the simulations, the director reorients in the (x, y) plane only for all the regimes explored in the present study. This allows us to fix $\Theta = \pi/2$ and the director is therefore fully described by the twist angle Φ. Finally, the strong boundary conditions in terms of the twist angle are

$$\Phi(z = 0, t) = \Phi(z = L, t) = 0. \tag{1}$$

3. 'TOFT' under ideal light field boundary conditions

Hereafter we shall use the normalised length $z \to z\pi/L$ and time $t \to t/\tau$ where $\tau = \gamma_1 L^2/(\pi^2 K_2)$ is a characteristic relaxation time with the rotational viscosity γ_1 and the twist Frank elastic constant K_2 [12].

In this section, we neglect the effect of the reflection of light at the boundaries $z = 0$ and $z = \pi$ and calculate the TOFT threshold by performing the linear stability analysis of the initially uniform planar orientational state. We eventually obtain the following integro-differential equation for Φ [10]:

$$\partial_t \Phi = \partial_z^2 \Phi + 2\rho\Delta^2 \left(\Phi + \Delta \int_0^z \Phi(z') \sin[\Delta(z' - z)] dz' \right), \tag{2}$$

where $\rho = I/I_c$ is the dimensionless incident light intensity with $I_c = 8\pi^2 c K_2 n_e \delta n/[\lambda^2(n_e + n_o)]$ and

$$\Delta = 2L\delta n/\lambda \tag{3}$$

is the reduced phase delay between e- and o-waves through the whole layer (in units of π)

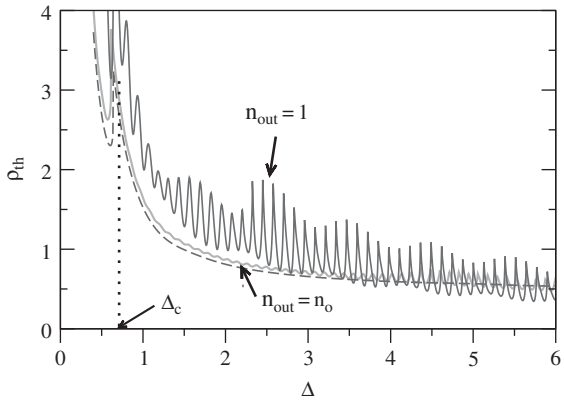

Figure 2. (Colour version online). Reduced twist optical Fréedericksz transition threshold ρ_{th} as a function of Δ with (solid lines) and without (blue dashed line) considering the effect of backward waves. Orange (light gray) line: refractive index of outer media $n_{out} = n_o$. Red (dark gray) line: $n_{out} = 1$. Lines with $\Delta < \Delta_c$ and $\Delta \geq \Delta_c$ correspond to stationary and Hopf bifurcation, respectively.

with birefringence $\delta n = n_e - n_o$, where n_e and n_o are the refractive indices of the o- and e-waves, respectively.

The linear stability analysis is performed by writing $\Phi(z,t) = \Phi(z)\exp(\sigma t)$ and inserting the spatial Fourier expansion

$$\Phi(z,t) = \sum_m \varphi_m(t)\sin(mz) \tag{4}$$

into Equation (2) with further projection on φ_n (the Galerkin method). The resulting eigenvalue problem is then solved numerically (see [10] for details). As a result, the value of the reduced twist optical Fréedericksz transition threshold, ρ_{th}, is determined.

The results are summarised by the blue dashed line in Figure 2 and the eigenvalue analysis shows that the primary instability of the planar state is a stationary bifurcation only below a critical value $\Delta = \Delta_c = 0.64$ and a Hopf bifurcation otherwise. We note that the change from stationary to Hopf bifurcation when Δ is taken as a control parameter is accompanied by a jump for the TOFT threshold, see Figure 2 and [10] for details.

4. 'TOFT' under realistic light field boundary conditions

Hereafter we consider realistic boundary conditions at $z = 0, \pi$, namely an isotropic dielectric material that sandwiches the nematic layer with refractive index n_{out}. For convenience, we introduce the labels i and t for the first ($z < 0$, incident side) and the second ($z > \pi$, transmitted side) semi-infinite surrounding dielectric material, and N for the nematic layer. The modified linear equation requires the derivation of the expressions for the o- and e-waves inside the nematic to the first order in that account for the backward wave contributions. This is done by using Berremen's formalism [18], when the Maxwell equations are cast in matrix form for the four-component vector $\bar{\Psi}^T = (E_x, H_y, E_y, -H_x)$. Here $\mathbf{E}(z,t)$, $\mathbf{H}(z,t)$ are the amplitudes of the electric and magnetic fields, $\mathbf{E}(\mathbf{r},t) = 1/2(\mathbf{E}(z,t)e^{-i\omega t} + \text{c.c.})$, $\mathbf{H}(\mathbf{r},t) = 1/2(\mathbf{H}(z,t)e^{-i\omega t} + \text{c.c.})$, where c.c. represents the complex conjugate, that vary slowly in time compared to ω^{-1}. The vector can be expressed by the superposition of four independent electromagnetic waves (two forward and two backward propagating) that propagates along z ($k_x = k_y = 0$) with the same frequency ω for i, t and N media (Oldano's formalism [19]), namely

$$\bar{\Psi} = \sum_{j=1}^{4} f_j \psi^j = f_1\psi^1 + f_2\psi^2 + f_3\psi^3 + f_4\psi^4 = \mathrm{T}\phi, \tag{5}$$

where T is the matrix whose columns are eigenvectors ψ^j and ϕ is the vector of amplitudes, $\phi^T = (f_1, f_2, f_3, f_4)$.

The vector of amplitudes ϕ at the left-hand side of the first boundary plane ($z = 0^-$) and at the right-hand side of the second boundary plane ($z = \pi^+$) can be written as

$$\phi^T(0^-) = (0, a_0, r_e, r_o),\ \phi^T(\pi^+) = (t_e, t_o, 0, 0). \tag{6}$$

The scattering problem consists of expressing the amplitudes r_e, r_o, t_e and t_o of the reflected and transmitted e- and o-waves as a function of the amplitude a_0 of the incident o-wave. The continuity of the tangential components of the vectors $\mathbf{E}$ and $\mathbf{H}$ at $z = 0, \pi$ requires

$$\bar{\Psi}(0^-) = \bar{\Psi}(0^+),\ \bar{\Psi}(\pi^-) = \bar{\Psi}(\pi^+), \tag{7}$$

so that we can write

$$\mathrm{T}_i\phi(0^-) = \mathrm{T}_N(0^+)\phi(0^+), \mathrm{T}_N(\pi^-)\phi(\pi^-) = \mathrm{T}_t\phi(\pi^+), \tag{8}$$

where T_i and T_t are as follows:

$$\mathrm{T}_i = \mathrm{T}_t = \frac{1}{\sqrt{2}} \begin{pmatrix} \frac{1}{\sqrt{n_i}} & 0 & \frac{1}{\sqrt{n_i}} & 0 \\ \sqrt{n_i} & 0 & -\sqrt{n_i} & 0 \\ 0 & \frac{1}{\sqrt{n_i}} & 0 & \frac{1}{\sqrt{n_i}} \\ 0 & \sqrt{n_i} & 0 & -\sqrt{n_i} \end{pmatrix}. \tag{9}$$

Owing to the boundary conditions for the director we have $\mathrm{T}_N(0^+) = \mathrm{T}_N(\pi^-) \equiv \mathrm{T}_N^0$ given by

$$\mathrm{T}_N^0 = \frac{1}{\sqrt{2}} \begin{pmatrix} \frac{1}{\sqrt{n_\mathrm{e}}} & 0 & \frac{1}{\sqrt{n_\mathrm{e}}} & 0 \\ \sqrt{n_\mathrm{e}} & 0 & -\sqrt{n_\mathrm{e}} & 0 \\ 0 & \frac{1}{\sqrt{n_\mathrm{o}}} & 0 & \frac{1}{\sqrt{n_\mathrm{o}}} \\ 0 & \sqrt{n_\mathrm{o}} & 0 & -\sqrt{n_\mathrm{o}}. \end{pmatrix}. \tag{10}$$

The evolution of the electromagnetic field as it passes through the nematic layer can be written by introducing the propagation matrix $\mathrm{K}(\pi)$ as

$$\phi(\pi^-) = K(\pi)\phi(0^+), \tag{11}$$

where

$$\mathrm{K}(\pi) = i\alpha\bar{k}_0 e^{i\pi\bar{k}_0 n_\mathrm{o}} \times \begin{pmatrix} \frac{e^{i\pi\bar{k}_0 d_1}}{i\alpha\bar{k}_0} & \xi_1 e^{i\pi\Delta} & 0 & \xi_2 e^{i\pi\Delta} \\ \xi_1 & \frac{1}{i\alpha\bar{k}_0} & -\xi_2 & 0 \\ 0 & -\xi_2^\star e^{-i\pi q\Delta} & \frac{e^{-i\pi q\Delta}}{i\alpha\bar{k}_0} & -\xi_1^\star e^{-i\pi q\Delta} \\ -\xi_2^\star e^{i\pi\Delta(1-q)} & 0 & -\xi_1 e^{i\pi\Delta(1-q)} & \frac{e^{i\pi\Delta(1-q)}}{i\alpha\bar{k}_0} \end{pmatrix}. \tag{12}$$

Here

$$\alpha = \frac{n_\mathrm{e}^2 - n_\mathrm{o}^2}{2\sqrt{n_\mathrm{e} n_\mathrm{o}}},\ q = \frac{n_\mathrm{e} + n_\mathrm{o}}{\delta n} \tag{13}$$

and

$$\xi_1 = \int_0^\pi e^{-i\Delta z}\Phi(z)dz,\ \xi_2 = \int_0^\pi e^{-i\Delta qz}\Phi(z)dz. \tag{14}$$

Finally, a set of four independent equations that allows us to express r_e, r_o, t_e and t_o as functions of a_0 is derived:

$$\phi(0^-) = \mathrm{T}_i^{-1}\mathrm{T}_N^0 K^{-1}(\pi)(\mathrm{T}_N^0)^{-1}\mathrm{T}_t\phi(\pi^+). \tag{15}$$

In general, the resulting expressions for the reflected and transmitted waves $r_\mathrm{e}, r_\mathrm{o}, t_\mathrm{e}$ and t_o are cumbersome. However it is instructive to consider the particular case $n_\mathrm{out} = n_\mathrm{o}$ that simplifies the algebra to a great extent and gives

$$\begin{aligned} r_\mathrm{e} &= \frac{ia_0 q\Delta \int_0^\pi \left[e^{i\Delta(\pi-z)} + qe^{-i\Delta q(\pi-z)}\right]\Phi(z)dz}{q^2 e^{-i\pi q\Delta} - e^{i\pi\Delta}}, \\ r_\mathrm{o} &= 0, \\ t_\mathrm{e} &= \frac{ia_0 q\Delta e^{\frac{i}{2}\pi\Delta(q-1)} \int_0^\pi \left[qe^{-i\Delta z} + e^{i\Delta qz}\right]\Phi(z)dz}{q^2 e^{-i\pi q\Delta} - e^{i\pi\Delta}}, \\ t_\mathrm{o} &= a_0 e^{-\frac{i}{2}\pi\Delta(q-1)}. \end{aligned} \tag{16}$$

As is expected, $r_\mathrm{o} = 0$ because an incident ordinary wave is perfectly matched ($n_\mathrm{out} = n_\mathrm{o}$). Thus, the o-wave is entirely transmitted acquiring only the phase according to Equation (16).

The light field distribution inside the nematic is then obtained by integrating the equations for the amplitudes $f_i(z)$, since the initial condition $\phi(0^+) = (\mathrm{T}_N^0)^{-1}\mathrm{T}_i(0, a_0, r_\mathrm{e}, r_\mathrm{o})^\mathrm{T}$ is known. Finally, the linearised expression for the electromagnetic term is calculated, leading to the following integro-differential equation for Φ:

$$\begin{aligned} \partial_t\Phi = \partial_z^2\Phi + 2\rho\Delta^2 \Bigg(\Phi + \Delta\int_0^z \Phi(z')\sin[\Delta(z'-z)]dz' \\ + \Delta\cdot\mathrm{Im}[F(z)]\Bigg), \end{aligned} \tag{17}$$

where $F(z)$ describes the contribution of the backward waves. Then, the stability analysis procedure is similar to the case of ideal boundary conditions (see Section 3). In the particular case $n_\mathrm{out} = n_\mathrm{o}$, the explicit formulation of the latter function is

$$\begin{aligned} F(z) = \int_0^z e^{-iq\Delta(z-z')}\Phi(z')dz' + \frac{(e^{i\Delta z} + qe^{-iq\Delta z})}{e^{i\pi\Delta} - q^2 e^{-i\pi q\Delta}} \\ \times \int_0^\pi \left[e^{i\Delta(\pi-z)} + qe^{-i\Delta q(\pi-z)}\right]\Phi(z)dz. \end{aligned} \tag{18}$$

The results are summarised in Figure 2 where the normalised TOFT threshold ρ_{th} is plotted as a function of the optical thickness of the planar nematic slab by taking Δ as the control parameter. The solid curves refer to the cases $n_{out} = n_o$ and $n_{out} = 1$ where the contribution of backward waves is taken into account. The dashed curve corresponds to the ideal case discussed in Section 3. The presence of backward waves has a clear qualitative effect: the TOFT threshold exhibits oscillations as a function of the normalised phase delay Δ of the nematic layer. Such an oscillation is driven by the dependence of the function $F(z)$ on Δ. In the case $n_{out} = n_o$, the resulting oscillation has a pseudo-period $2/q$ (see Equation (18)). This corresponds to a pseudo-period of $\lambda/(n_e + n_o)$ when considering the dependence of the threshold on the thickness L. Such a behaviour emphasises the role played by the interference between forward and backward propagating waves, to which we can attribute the physical origin of the modulation of the TOFT threshold. Accordingly, the modulation depth drastically increases when the refractive index jump at the nematic boundaries is increased, as shown in the case $n_{out} = 1$ (see Figure 2).

Intriguingly, we note that the TOFT threshold is found to exhibit strong relative variations (typically up to 100%, see Figure 2) although the refractive index mismatch is associated with modest intensity reflectance (of the order of a few percent). This indicates the crucial role played by the spatially distributed optical feedback inside the liquid crystal rather than the intensity spatial modulation inside the nematic which is only due to light field reflections on the cell boundaries, i.e. without liquid crystal reorientation. In fact, to grasp some qualitative understanding of the optical feedback issue from the light intensity distribution one should instead have a look at the situation at the onset of the reorientation process. This implies solving the full numerical problem — a task that departs from our approach developed here since we merely solve the eigenvalue problem for the determination of the threshold ρ_{th} as a function of Δ. Nevertheless, our approach clearly allows us to emphasise under what conditions the effect of seemingly negligible backward scattering can have a significant impact.

Moreover, it turns out that the TOFT threshold can be larger or lower than in the ideal case depending on the value of the phase delay (see Figure 2). This should certainly be related to the wavelength dependence of the threshold in the presence of backward waves. Such a dependence is indeed known to be complex, as discussed in a recent work [6] where the effect of backward waves is prominent since the planar nematic is inserted into a one-dimensional periodic structure. In that case, it was shown that the TOFT threshold can even be larger than the perfectly matched situation [6], which offers a valuable hint to explain the predicted non-intuitive effect.

It is worth noting that relatively high values for TOFT could be drastically reduced, thereby becoming possibly accessible experimentally, by embedding the nematic liquid crystal layer into a periodic dielectric structure. Indeed, in such a case, the nematic is an optically nonlinear defect layer for the corresponding one-dimensional photonic structure. The reasoning behind this is that the Bragg scattering mechanism allows the light field to accumulate within the nematic cell at the so-called defect mode frequencies, thereby possibly lowering the TOFT threshold by orders of magnitude [6].

Finally, we conclude this section by an experimental remark noting that a sample is typically made of a nematic slab sandwiched between two glass substrates (with refractive index $n_{glass} \simeq n_o$) surrounded by air. Therefore, we expect the air/glass interfaces to control the modulation of the TOFT threshold, which therefore corresponds qualitatively to the case $n_{out} = 1$.

5. Conclusions

The effect of backward and forward scattering on the optical Fréedericksz transition threshold in a nematic layer with uniform planar alignment has been investigated. The optical thickness of the liquid crystal layer has been found to be the key parameter. In particular, we have shown that the reorientation threshold intensity oscillates as a function of the optical thickness, an effect which is especially pronounced in the presence of the refractive index mismatch at the film boundaries.

References

[1] Tabiryan, N.V.; Sukhov, A.V.; Zel'dovich, B.Y. *Mol. Cryst. Liq. Cryst.* **1986**, *136*, 1–139.

[2] Demeter, G.; Krimer, D.O. *Phys. Reports* **2007**, *448*, 133–162.

[3] Khoo, I.C. *Phys. Reports* **2009**, *471*, 221–267.

[4] Miroshnichenko, A.E.; Brasselet, E.; Kivshar, Y.S. *Phys. Rev. A: At., Mol., Opt. Phys.* **2008**, *78*, 053823(1)–053823(11).

[5] Miroshnichenko, A.E.; Brasselet, E.; Kivshar, Y.S. *Appl. Phys. Lett.* **2008**, *92*, 253306(1)–253306(3).

[6] Miroshnichenko, A.E.; Brasselet, E.; Krimer, D.O.; Kivshar, Yu.S. *J. Opt.* **2010**, *12*, 124006(1)–124006(8).

[7] Gusev, I.V.; Zel'dovich, B.Ya.; Krivoshchekov, V.A.; Sadovskii, V.N. *JETP Lett.* **1992**, *55*, 178–183.

[8] Khoo, I.C.; Diaz, A. *Phys. Rev. E: Stat., Nonlinear, Soft Matter Phys.* **2003**, *68*, 042701(1)–042701(4).

[9] Santamato, E.; Abbate, G.; Maddalena, P.; Shen, Y.R. *Phys. Rev. A: At., Mol., Opt. Phys.* **1987**, *36*, 2389–2392.
[10] Krimer, D.O. *Phys. Rev. E: Stat., Nonlinear, Soft Matter Phys.* **2009**, *79*, 030702(R)(1)–030702(R)(4).
[11] Laudyn, U.A.; Miroshnichenko, A.E.; Krolikowski, W.; Chen, D.F.; Kivshar, Yu.S.; Karpierz, M.A. *Appl. Phys. Lett.* **2008**, *92*, 203304(1)–203304(3).
[12] de Gennes, P.G.; Prost, J. *The Physics of Liquid Crystals*; Clarendon Press: Oxford, 1993.
[13] Krimer, D.O.; Demeter, G.; Kramer, L. *Phys. Rev. E: Stat., Nonlinear, Soft Matter Phys.* **2005**, *71*, 051711(1)–051711(10).
[14] Demeter, G.; Krimer, D.O.; Kramer, L. *Phys. Rev. E: Stat., Nonlinear, Soft Matter Phys.* **2005**, *72*, 051712(1)–051712(4).
[15] Brasselet, E.; Galstian, T.V.; Dube, L.J.; Krimer, D.O.; Kramer, L. *J. Opt. Soc. Am. B* **2005**, *22*, 1671–1680.
[16] Krimer, D.O.; Kramer, L.; Brasselet, E.; Galstian, T.V.; Dube, L.J. *J. Opt. Soc. Am. B* **2005**, *22*, 1681–1690.
[17] Ledney, M.F. *JETP Lett.* **2007**, *85*, 328–330.
[18] Berreman, D.W. *J. Opt. Soc. Am. B* **1972**, *62*, 502–510.
[19] Oldano, C. *Phys. Rev. A: At., Mol., Opt. Phys.* **1989**, *40*, 6014–6020.